

On the non-destructive detection of fatigue damage in industrial aluminium alloys by positron annihilation

Uwe Holzwarth · Petra Schaaff

Received: 12 June 2006 / Accepted: 22 September 2006 / Published online: 4 April 2007
© Springer Science+Business Media, LLC 2007

Abstract The average positron lifetime has been determined non-destructively and in-situ during fully symmetric push-pull fatigue experiments in the bulk material of the aluminium alloys 2024 T3 and 7075 T6 using a servo-hydraulic fatigue testing system equipped with a mobile positron beam produced by a $^{72}\text{Se}/^{72}\text{As}$ generator (initial activity of ≈ 0.9 MBq; average positron penetration depth ≥ 1 mm). Contrary to earlier investigations on stainless steel using the same experimental approach, no variation of the average positron lifetime could be observed during fatigue and neither early nor late stages of fatigue damage could be revealed. It is concluded that fatigue induced changes of the defect spectra in technologically relevant aluminium alloys are masked for the present method by saturation trapping in precipitates. A sufficiently high increase of the dislocation density and the creation of vacancy clusters must be confined to the vicinity of propagating fatigue cracks or the fatal fatigue crack. Therefore the zone with sufficient detectable fatigue damage has not enough statistical weight to modify the average positron lifetime of the aluminium alloy bulk material.

Introduction

Positron annihilation is highly sensitive to open volume defects like vacancies, vacancy clusters and dislocations introduced by plastic deformation or misfit dislocations at the interface between semi- or non-coherent precipitates and the surrounding matrix. Even coherent precipitates that do not offer open volumes may be efficient positron trapping sites provided the positron affinity to the constituting atoms is higher than that to the matrix [1]. Positrons trapped in such precipitates that exceed a critical size exhibit the specific positron lifetime in the corresponding intermetallic phase [2]. Comprehensive presentations of the physical basis of positron annihilation techniques can be found in the reviews e.g. by Nieminen and Maninen [3], Schulz and Lynn [4] and Puska and Nieminen [5]. In iron and steels it has been demonstrated that the high sensitivity of positron annihilation can be exploited to non-destructively detect early stages of fatigue, to monitor the evolution of fatigue damage and to attempt a non-destructive residual lifetime prediction [6–10]. In aluminium alloys positron annihilation methods contributed significantly to the understanding of the complex precipitation processes and precipitation kinetics that occurs in aluminium alloys during natural and artificial aging [11–15].

In spite of the high mobility of atomic defects in aluminium, progressing tensile deformation has successfully been detected in positron annihilation studies in pure aluminium [16–19]. Recent investigations demonstrated the feasibility to study the initiation and growth of fatigue cracks in fracture toughness specimens fabricated from the industrial aluminium alloys 2024 [20] and 6013 [20–22] using positron micro-beams with a spatial resolution between $2\ \mu\text{m}$ [21, 22] and $20\ \mu\text{m}$ [20, 22]. In this way the plastic zone around the crack tip could be imaged using the

U. Holzwarth (✉) · P. Schaaff
Institute for Health and Consumer Protection, European
Commission, Joint Research Centre, Via E. Fermi 1 (T.P. 500),
Ispra, VA 21020, Italy
e-mail: uwe.holzwarth@jrc.it

Present Address:
P. Schaaff
Società Italiana Brevetti, Via Carduzzi 8, Milano 20123, Italy

doppler broadening of the 511 keV annihilation line [20] or the positron lifetime [21, 22] as imaging parameter. There are however no results available in literature that describe the effect of progressing fatigue damage on the evolution of the average positron lifetime of the bulk material as it has been reported for stainless steel [6, 8].

Contrary to pure aluminium, most technologically interesting alloys (series 2XXX, 6XXX, 7XXX) are hardened by high densities of nano-sized precipitates that consequently provide a high density of various positron trapping sites that could well mask the effect of a minor concentration of additionally produced positron traps during fatigue. Indeed, the heavy plastic tensile deformation applied to the superplastic, predominantly solution hardened, aluminium alloy 5083 by Araki et al. [23], the thickness reduction by cold rolling applied on the annealed alloys 2024 [24] and 7075 [25] and the axial tensile straining applied to various Al–Li alloys [26] show a very moderate increase of the average positron lifetime compared to materials such as stainless steel [6, 8], iron [7, 19] or copper [27]. However, just due to the complex microstructure of aluminium alloys, the effect of fatigue on the average positron lifetime in the bulk is difficult to predict. Therefore, the present investigation made an attempt to apply a technique to non-destructively follow the fatigue damage evolution, which has already been applied successfully to stainless steel AISI 316L [6, 28] and copper [27, 29], to technologically relevant aluminium alloys.

Two points were in favour of this attempt. Firstly, aluminium and its alloys exhibit a matrix with face-centred cubic crystal structure that is prone to the formation of persistent slip bands during fatigue [30, 31]. If plastic strain gets localized in such slip bands they exhibit a large turnover of dislocations and atomic defects [32] by continuous production, motion and annihilation of dislocations and dislocation dipoles, leading also to the formation of clusters of atomic defects [33, 34], thereby changing the microstructure and consequently the densities of positron traps in a way that an effect on the average positron lifetime should be measurable. Moving dislocations can also cut through and segment precipitates in aluminium alloys [35, 36] causing material softening. In strain-controlled experiments the crystal volume of these persistent slip bands increases above a threshold value of the plastic strain amplitude from zero up to 100% [30]. At least in stress-controlled fatigue experiments at high stress amplitudes strain localization and microstructural changes should be expected that are detectable by positron annihilation. Secondly, the $^{72}\text{Se}/^{72}\text{As}$ positron generator used in the present investigation emits two positron spectra with maximum energies of 2.5 MeV and 3.3 MeV. The positrons with the most probable energy in the spectra (about a third of the maximum energy) penetrate about 1 mm and 1.5 mm into

aluminium. Therefore the volume contributing to the signal is quite large and real bulk properties of the material are revealed.

The choice of the aluminium alloys 2024 and 7075 in the temper conditions T3 and T6, respectively, was motivated by the importance of these alloys for aeronautic industry. The experiments started with the alloy 2024 deformed at sufficiently high stress amplitudes to provoke microstructural changes due to strain localization in a significant portion of the grains. It will be shown that no significant change of the average positron lifetime was observed in contrast to similar experiments on stainless steel AISI 316L. This led to a change of the experimental strategy, i.e., to examine fatigue specimens post-mortem, i.e., after failure that had been used in an earlier investigation to establish the Wöhler curves for various alloys. In this way the average positron lifetime was determined after failure as a function of the applied stress amplitudes for various aluminium alloys. In contrast to austenitic stainless steel that exhibits a pronounced increase of the positron lifetime after failure with increasing stress amplitude for each aluminium alloy a practically constant value was found for all applied stress amplitudes.

Experimental procedures

Materials, specimen preparation and fatigue testing

The compositions of the investigated aluminium alloys as given by the supplier certificates are compiled in Table 1. The temper states in which the aluminium alloys were purchased and the temper procedures are compiled in Table 2. The alloys were purchased in form of rods of 30 mm diameter and a few meters length. From these rods pieces of 170 mm were cut and cylindrical fatigue specimens were machined according to the procedure described in the standard ASTM E 466 and ASTM E 606 of the American Society for Testing and Materials [37]. In this way on the central gauge length of 30 mm length with a diameter of 10 mm a final surface roughness of better than 0.25 μm was obtained (cf. specimen shape Type A in Fig. 1 of reference [6]). Specimen shape and the execution of the fatigue tests complied with the ASTM Standard E 466 (“Conducting Constant Amplitude Axial Fatigue Tests of Metallic Materials”) and ASTM Standard E 606 (“Standard Recommended Practice for Low-Cycle Fatigue Testing”) [37].

The aluminium alloys were cyclically deformed in stress-controlled experiments. The uniaxial stress σ was calculated from the axial force F , measured by a load cell, divided by the cross sectional area A of the specimen on the gauge length. The fatigue experiments were performed in a

Table 1 Chemical composition of the investigated aluminium alloys according to supplier information. The main alloying elements are highlighted

Alloy	Composition in weight (%)									
	Cu	Mg	Zn	Fe	Si	Mn	Ti	Cr	Zr	Al
2017	4.07	0.70	0.11	0.34	0.42	0.69	0.01	0.06	0.00	balance
2024	4.03	1.29	0.12	0.33	0.34	0.74	0.01	0.07	0.00	balance
5154	0.05	3.37	0.08	0.39	0.28	0.31	0.08	0.25	0.00	balance
6060	0.01	0.67	0.01	0.31	0.75	0.50	0.01	0.02	0.00	balance
7075	1.38	2.38	5.75	0.36	0.19	0.23	0.04	0.22	0.01	balance

closed-loop controlled servohydraulic material test system (MTS 810) that compares the measured current value $\sigma(t)$ with the sinusoidal command signal supplied by a function generator. The difference between both signals is used as error signal to command the hydraulic actuator. In this way the stress in the material follows the shape of the command wave. Symmetric push-pull fatigue experiments ($\sigma_{\min}/\sigma_{\max} = -1$) were performed at a frequency of 1 Hz for experiments with on-line positron lifetime measurements and at 10 Hz for the specimens used for the determination of Wöhler curves and post-mortem positron lifetime measurements.

Positron lifetime measurements

A mobile positron beam has been mounted to the load frame of the fatigue machine that allowed to perform repeated positron-lifetime measurements in the center of the gauge length without removing the specimen from the load train. Deviating from the procedure applied in the case of stainless steel where fatigue cycling was paused after

100, 200, 500, 1000, 2000, 5000, 10000 cycles and so on in logarithmic sequence [6] the tests aiming at the observation of fatigue damage evolution in the aluminium alloys were run in continuous mode. This means that positron annihilation spectra were recorded during fatigue. After accumulating 10^6 coincidence events a new spectrum was recorded. This variation of the method was applied in order to allow positron trapping also into defects like single vacancies that are mobile at room temperature and vanish rapidly by annealing. The last measurements were performed after failure of the specimens. Three experiments have been performed in this mode on the alloy 2024 with applied stress amplitudes of 180 MPa, 210 MPa and 250 MPa. Later on, only post-mortem measurements were performed on specimens of various aluminium alloys that underwent earlier fatigue testing until failure in order to establish the fatigue limit of the materials by recording Wöhler curves.

Table 2 Thermal treatments of the investigated materials according to supplier information

Alloy	Treatment	Treatment details
2017	T4	Extruded rod, solution heat treated at 500 °C for 1 h, natural aging at 20 °C for 120 h
2024	T3	Extruded rod, solution heat treated at 500 °C for 1 h, cold worked, natural aging at 20 °C for 120 h
5154	H34	annealed, cold rolled and stabilization temper
6063	T6	Extruded rod, solution heat treated at 530 °C for 1 h, artificially aged at 150 °C for 24 h
7075	T6	Extruded rod, solution heat treated at 470 °C for 2 h, artificial aging at 120 °C for 24 h

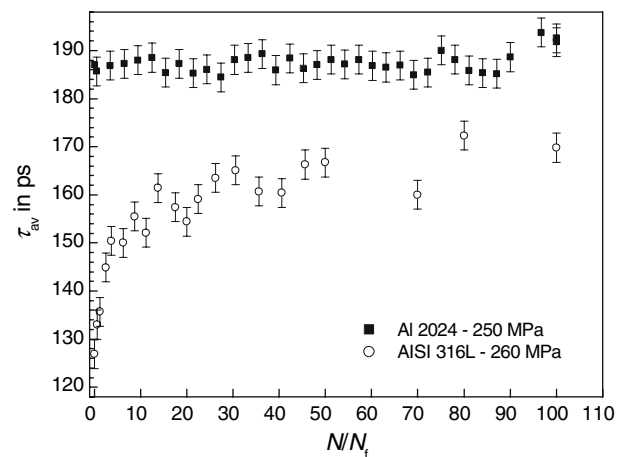


Fig. 1 Comparison of the evolution of average positron lifetime τ_{av} during stress-controlled fatigue experiments between stainless steel AISI 316 L and the aluminium alloy 2024. The number of fatigue cycles N is normalized to number at failure N_f . For the comparison the stress amplitudes for the aluminum alloy and the stainless steel have been selected to have similar fatigue life N_f . The error bars denotes the accuracy of the positron lifetime measurement of ± 3 ps

The experimental set-up of the mobile positron beam and the production of the miniaturized positron sources used for the present experiments has been described in detail elsewhere [6, 27, 29]. A $^{72}\text{Se}/^{72}\text{As}$ generator with a maximum initial activity of about $25 \mu\text{Ci}$ ($\approx 0.9 \text{ MBq}$) was used as positron source. ^{72}As emits two positron spectra with maximum energies of 2.5 MeV and 3.3 MeV. The ^{72}Se was vapour deposited inside a small gold cylinder of 0.6 mm inner diameter acting as beam collimator. This gold cylinder was integrated in the tip of a plexiglass light guide on top of a photomultiplier tube. The source was covered by a plastic scintillator which produces a scintillation start signal only for those positrons which are emitted in the direction towards the specimen under examination. The stop signal was delivered by a BaF_2 crystal after registration of the 511 keV annihilation quanta. Signal processing was done by a fast-slow coincidence measurement as described earlier [27, 29]. The time resolution of the instrument has been determined as of (230 ± 5) ps by fitting a Gaussian curve to the 835 keV prompt (3 ps) line emitted from the ^{72}Ge after the emission of a 2.5 MeV positron by the ^{72}As .

Compared with the sandwich technique using a ^{22}Na source the present technique exploits a much smaller solid angle. The effect on count rate is however largely compensated by the higher detection efficiency of the β - γ -coincidence as compared to the γ - γ -coincidence. During the positron-lifetime measurements the specimens were shielded with plexiglass capturing all positrons that missed the specimen or were reflected from its surface. The mean positron lifetime in plexiglass of about 1500 ps, mainly determined by the pick-off annihilation of the positron triplet state [29], is sufficiently different from the mean positron lifetimes in a metal of 100–300 ps that an easy background correction could be performed by weighted subtraction of a plexiglass reference spectrum. The weighting factor was determined from the ratio of counts in a window of the spectrum in which the spectrum was determined by very long-lived contributions only (≥ 1000 ps), and the counts in the same window in the reference spectrum. This method corrects also the annihilation events of low energy positrons in the scintillation start detector as well as possible tiny contributions of short-lived components in the plexiglass spectrum that could interfere with long positron lifetime components in fatigued alloys. Before correction each spectrum contained 1.0×10^6 coincidence events. The required acquisition time increased from about 20 min initially to more than 2.5 h after 4 weeks due to the short half-life of the $^{72}\text{Se}/^{72}\text{As}$ generator. Typically 55% of these events were lost by the background correction. The average positron lifetime was evaluated by a weighted linear regression to the linear part of the spectrum in logarithmic presentation. The statistical

error of the fits are less than 1 ps. The overall accuracy is ± 3 ps and is determined by the reproducibility of repeatedly recording and evaluating a spectrum of the same specimen. The statistics after background correction is not sufficient for a decomposition of the mean positron lifetime into different components. At least twice the number of coincidence events are recommended for a stable decomposition in more lifetime components [38].

Results

In Fig. 1 the typical evolution of the average positron lifetime τ_{av} of a AISI 316L stainless steel specimen, taken from an earlier investigation [6], is compared with those obtained in the present investigation on the aluminium alloy 2024. The number of fatigue cycles N is normalized in both cases to the number of cycles at failure N_f . The stress amplitudes that have been selected for comparison result in roughly the same fatigue life N_f for both materials of $\leq 100,000$ cycles. It is evident that τ_{av} does not change during the fatigue life of the aluminium alloy 2024 specimen in spite of the rather high applied stress amplitude of 250 MPa. A practically constant average positron lifetime of $\tau_{\text{av}} = (187 \pm 3)$ ps has been determined throughout the fatigue experiment for all tested stress amplitudes. The same value of τ_{av} was obtained on annihilation spectra irrespectively whether they were recorded on-line during fatigue, with the method applied on stainless steel, i.e., pausing the experiments for recording the spectra and when the pauses were extended to some hours before recording the positron annihilation spectra. After failure the measurements could be repeated after several months with the same results for τ_{av} .

The same behaviour was found for the aluminium alloy 7075 cyclically deformed at 260 MPa. In order to minimize effort only a few spectra were recorded that gave enough evidence for the same flat curve of τ_{av} versus N . Figure 2 summarizes the sensitivity of positron lifetime measurements to fatigue damage. In stainless steel there is a pronounced tendency of τ_{av} to increase during fatigue until failure, which is completely absent in the aluminium alloys 2024 and 7075.

With these results the initial measurement programme was abandoned because it became clear that a stress dependent differentiation in the evolution of the average positron lifetime as obtained on stainless steel could not be verified in the aluminium alloys 2024 and 7075. In an attempt to get a quick overview on the positron annihilation behaviour in fatigued aluminium alloys a series of measurements was performed on failed specimens of the aluminium alloys 2017, 2024, 5154, 6060 and 7075 that had been cyclically deformed for an earlier study on aluminium

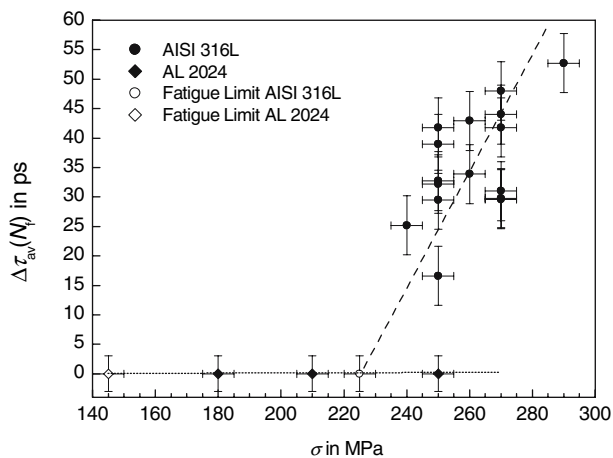


Fig. 2 The distinctly different behaviour of the two material groups is reflected in the increase of the average positron lifetime $\Delta\tau_{av}(N_f)$ during stress-controlled fatigue experiments until failure as a function of the applied stress amplitude σ . The open symbols define the fatigue limits of the materials

alloys that included a check of the fatigue limit of the alloys by recording their Wöhler curves. These Wöhler curves and the results of the measurements of $\tau_{av}(N_f)$ after failure at N_f fatigue cycles as a function of the applied stress amplitude σ are reported in Figs. 3 and 4, respectively. From these measurements it is obvious that there is no significant dependence of the average bulk positron lifetime measured after failure, $\tau_{av}(N_f)$, for the aluminium alloys 2024 and 7075. Within the uncertainty of τ_{av} of ± 3 ps and in view of the scatter inherent to fatigue experiments the slight tendency towards increased values for $\tau_{av}(N_f)$ on the alloys 2017 T4 and 5154 H34 appears too weak to be useful for non-destructive testing purposes.

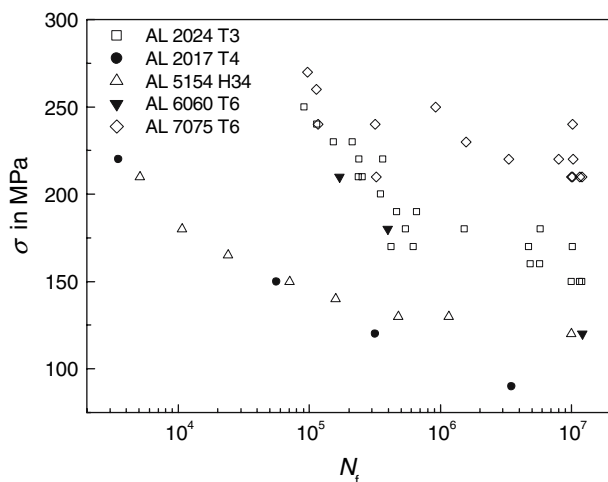


Fig. 3 Wöhler curves of the aluminium alloys 2024 and 7075. Included are also data of the aluminium alloys 2017, 5154 and 6060. σ denotes the applied stress amplitude in symmetric push-pull fatigue tests (stress ratio $\sigma_{min}/\sigma_{max} = -1$) and N_f is the number of fatigue cycles to failure (fatigue life)

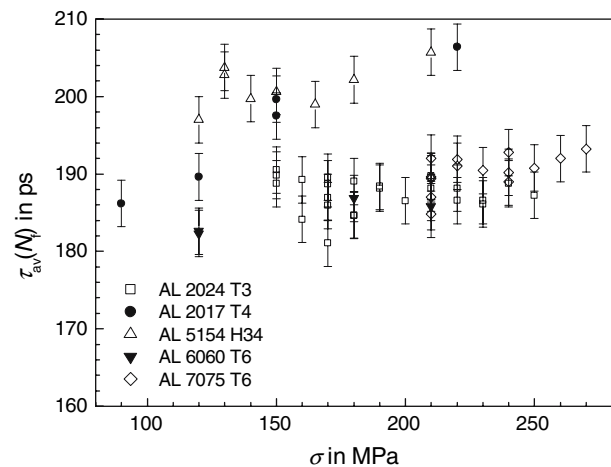


Fig. 4 Average positron lifetime after failure $\tau_{av}(N_f)$ determined on the specimens presented in Fig. 3. The presentation confirms the observations presented in Fig. 1 that there is no effect of the stress amplitude σ on the average positron lifetime.

Discussion

The most striking and most important finding of the present investigation is that it is not possible to monitor the evolution of fatigue damage in aluminium alloys by determining the average positron lifetime with the method that looks so promising for austenitic stainless steel. In stainless steel [6, 8, 9] and ferritic steel [9, 39] positron annihilation is sensitive to a microstructure change that affects the whole bulk of the fatigued material, whereas in aluminium alloys positron trapping in a high density of precipitates masks the effect of fatigue with the exception of a confined zone around the propagating crack tip, which can be detected by microbeam techniques with high spatial resolution [20–22]. The significant increase of positron lifetime around a crack tip in Al 6013 from 216 ps to 240 ps [11] has been explained by a transition from trapping into Mg-rich precipitates to trapping into dislocations and vacancy clusters created by dislocation processes in the vicinity of the crack tip [11, 22]. If fatigue damage that is detectable by positron lifetime measurements is confined to the area in front of the propagating fatal fatigue crack, it is however unlikely to capture this volume element by the present bulk measurement on a cylindrically shaped fatigue specimen since, in contrast to fracture toughness specimens, the geometry of cylindrical fatigue specimens does not define a preferential site for the development of the fatal crack within the gauge length. Even if captured accidentally, its statistical contribution to the volume probed by the positrons will probably be too low. In stainless steel the fatigue induced increase of the average positron lifetime in the whole cyclically stressed and strained volume allows to follow the evolution of fatigue damage without prior knowledge of where the fatal crack will develop.

Table 3 Compilation of positron lifetimes τ_{trap} for specific trapping sites identified in different aluminium alloys classes and the observed range of the average positron lifetime, τ_{av} , as reported in literature for various treatment conditions (GPZ denotes Guinier–Preston-Zones)

Alloy	Positron trap	τ_{trap}	Source	Range of τ_{av} in literature
Al2024	θ' (Al_2Cu) phase	192 ps [40]		212–186 ps depending on aging time at 190 °C after solution annealing (5 h, 483 °C), water quenching, preaging at 20 °C for 72 h and tensile deformation at 62 °C [41]; with modified treatment parameters: 212–178 ps [14];
	S' (Al_2CuMg) phase	240 ps [40]		210–186 ps [42] and 207–192 ps [43]
	GPZ containing a vacancy	177 ps [14]		
Al5083	–	–	–	161 ps fully annealed, increasing to 218 ps after cold rolling and decreasing to 203 ps after superplastic deformation [23]
Al6013	Mg-rich precipitates dislocations and/or small	216 ps [11]		216 ps in annealed (“as received”) state [11]
	vacancy clusters	240 ps [22]		240 ps around a propagating crack tip [11, 22]
Al7012	GPZ	155 ps [40]		203 ps after solution annealing (2 h; 475 °C), quenching to 20 °C, preaging (5 d; 20–45 °C) and aging for 2000 min at 180 °C [44]
	GPZ associated with vacancy	220 ps [40]		
Al7075	(Al–Zn) $\alpha'R\gamma'$ phase	240 ps [40]		between 189 ps after 3 h annealing at 320 °C and 214 ps after 3 h annealing at 240 °C following solution annealing (5 h at 500 °C) and water quenching [42]
	(Al–Zn–Mg) η' Zn ₂ Mg phase	240 ps [40]		

The determined τ_{av} values for the alloys are rather low compared with literature data (see Table 3 [11, 14, 22, 23, 40–44]) and nourished some doubts about the evaluation procedure and the background correction. However, various attempts to vary the width and the position of the windows on the spectra for the linear regression and the background correction resulted only in a linear shift of the τ_{av} values by 3–5 ps. There were no indications on a so far undiscovered, hidden tendency in the positron lifetime data.

Various studies on the precipitation kinetics during aging report that in aluminium alloys there is apparently no trapping and annihilation in dislocations [20, 26, 41] since the positron affinity to precipitates is much higher. The high density of vacancies that are produced by fatigue especially in areas of strain localization are efficient positron traps. However, they are mobile in the aluminium matrix at room temperature [45, 46]. Therefore they contribute to the annealing of dislocations by climb which is an

efficient way of consumption of atomic defects. Only those will survive that create solute vacancy complexes or that are themselves trapped in or by precipitates. The great variety of positron traps that may contribute to the positron lifetime spectra in aluminium alloys and their specific positron lifetimes have been classified and compiled by Dlubek et al. [40, 42, 47]. The $\tau_{\text{av}}(N = 0)$ values determined for the aluminium alloys used in the present study (see Table 4) are roughly within the limits reported in literature, whereas the mechanical properties correspond to the expectations [48, 49]. The values for $\tau_{\text{av}}(N = 0)$ do not correspond to the specific lifetime of a certain positron trap. Therefore, under the assumption that saturation trapping is maintained during fatigue, various traps related to precipitates must contribute to the average positron lifetime with approximately constant statistical weight. Moreover, none of the dominant trapping sites are significantly modified during fatigue e.g. by capturing fatigue induced vacancies.

Table 4 Mechanical alloy properties according to supplier information: critical yield stress at 0.2% elongation, $\sigma_{0.2}$, maximum yield stress, σ_m , elongation at σ_m , fatigue limit at 1×10^7 cycles, and average positron lifetime $\tau_{\text{av}}(N = 0)$ in the as received state, before fatigue ($N = 0$)

Alloy and state	$\sigma_{0.2}$ in MPa	σ_m in MPa	ϵ_m in %	Brinell Hardness	Fatigue limit in MPa	$\tau_{\text{av}}(N = 0)$ in ps
2024 T3	508	571	11	–	150 ± 10	193 ± 3
2017 T4	230	380	10	105	80 ± 10	187 ± 3
5154 H34	228	295	12	74	120 ± 10	191 ± 3
6060 T6	185	230	12	–	120 ± 10	184 ± 3
7075 T6	485	625	7	145	190 ± 10	189 ± 3

One of the problems comparing the present positron lifetimes on industrially produced material batches with literature data is the incomplete knowledge of the processing parameters. For commercially purchased alloys, parameters like temperature homogeneity, quenching rates and natural aging, which may continue as “shelf aging”, are less controlled than in laboratory experiments that are especially designed to investigate precipitation sequences. Especially quenching rates are poorly defined since they depend on the batch size and geometry of the treated material and not only on the temperature difference between the material and the quenching medium. Moreover quenching rates are likely to vary with the distance from the material surface in a quenched piece. In many investigations also the composition of the alloys is restricted to the components of Guinier–Preston zones and intermetallic particles of known composition thereby controlling much better the content of impurities. A comparison with recent studies [11–15] indicates that the variation bands of the thermal and mechanical treatment parameters tolerated in industry for temper treatments such as T3, T4 or T6 [48] are large enough to cause significant differences in the measured average positron lifetime. The present materials have been supplied in a state that can essentially be considered as stable, as requested and used by industry. Table 2 compiles the treatment parameters as far as the details could be retrieved from the suppliers.

The τ_{av} values for the alloys 2017 and 2024 can be discussed together since both are Al–Cu–Mg alloys. In the as received, naturally aged state values of 193 ± 3 and 187 ± 2 were determined, respectively. Staab et al. [43] reported a lifetime of 208 ps in their naturally aged 2024 specimens and a decrease over up to 40 years due to continuing natural aging. For different thermal treatments of Al–Cu–Mg alloys the literature data range between 182 ps [14] and 212 ps directly after solution annealing and quenching to room temperature [14, 41]. The present τ_{av} values are rather on the lower limit and are usually obtained only after artificial aging at temperatures well above room temperature [14, 41]. In all laboratory experiments the duration of the homogenization or annealing treatment at a temperature between 482 °C and 500 °C is between 2 and 10 h, which is much longer than the one 1 h in the present case [13, 14, 41, 50, 51]. Moreover, the straining required for the T3 state has been performed only in two investigations [41, 51]. If we assume saturation trapping with $\tau_{av} \approx 190$ ps the candidates are semi-coherent precipitates of the θ' (Al₂Cu) and S' (Al₂CuMg) phases with specific positron lifetimes of 192 ps and 240 ps, respectively [40], with a necessary contribution of trapping in copper-rich precipitates, Guinier–Preston zones or clusters containing a vacancy [14] to which a lifetime of 177 ps has been assigned [52]. Ferragut and Somoza [41]

pointed out that misfit regions compete with Guinier–Preston–Bagaryatskii zones and clusters as trapping sites, whereas single vacancies disappear too quickly to be detected, and in spite of high dislocation densities trapping into dislocations does not contribute to the spectrum because the positron affinity to other structural defects is much higher.

For the alloy 7075 which is of Al–Zn–Mg type Dlubek et al. [42] reported a positron lifetime of 210 ps after isochronal annealing for 3h, and a minimum of 189 ps after annealing at 320 °C. In the alloy 7012, Somoza [44] reported a positron lifetime of 212 ps after artificial aging. In both cases however, the aging temperatures were at least 150 °C and hence higher than in the present case. Also the compositions of the alloys differ from our's. Other differences like pre-aging at room temperature may affect the positron lifetime too. Macchi et al. [12] reported average positron lifetimes after annealing at 460 °C for 2 h and artificial aging at 150 °C for 24 h of about 206 ps that decreased towards 202 ps after one week at room temperature. This was the treatment closest to the present T6 temper found in literature. Also in this case the values found in the present investigation are slightly lower than in literature, however, the composition of the alloy used by Macchi et al. [12] is quite different from 7075 as it contains less Zn, more Mg and nearly no further impurities. An intentionally introduced Ag impurity caused a decrease of the positron lifetime to 196 ps after one week at room temperature. Following Dlubek et al. [40] the potential positron traps are coherent Guinier–Preston-Zones without vacancies, with associated vacancies, and semi-coherent precipitates of the $\alpha'R\gamma'$ and $\eta'Zn_2Mg$ phases with positron lifetimes of 155 ps, 220 ps, 240 ps and 240 ps, respectively. Hence, in the present case the dominating contribution must be trapping in coherent Guinier–Preston-Zones without vacancies.

No literature data could be found concerning positron lifetimes in the aluminium alloy 5154. For the most similar alloy of the 5XXX series examined by positron annihilation, the alloy 5083 [23] with the composition 4.7Mg-0.65Mn-0.13Cr, average positron lifetimes of 161 ps in the fully annealed state, 218 ps after cold rolling and 203 ps after superplastic deformation at high temperature have been reported, which is however too unspecific for any comparison. Also no data are available on the average positron lifetime in the alloy 6060. Only a value of 216 ps, attributed to positron trapping in Mg-rich precipitates, has been reported by Dupasquier et al. [11] for the alloy 6013 T6 of the 6XXX family. Due to the strong influence of composition and thermal and mechanical treatment on the microstructure and hence on the density of positron traps, we can only conclude that the τ_{av} values obtained in the present study are on the

lower side of the range found in literature, but still appear reasonable.

It is beyond the scope of the present paper to review the trapping behaviour of positrons in precipitation hardened aluminium alloys. But taking into account (i) the typical densities of nanometer-sized precipitations (3–7.5 nm in the alloy 7075 T6) in the range between $5 \times 10^{19} \text{ m}^{-3}$ [53] and about $3 \times 10^{23} \text{ m}^{-3}$ [54], corresponding to a particle separation of some 10 nm, and (ii) the diffusion length of positrons in defect-free aluminium of about 400 nm [43] and (iii) the precipitates being formed by alloying elements having a significantly higher positron affinity than the matrix [1] it is reasonable to assume that even high dislocation densities cannot compete with precipitates as trapping sites. For non-destructive testing purposes unfortunately also the large amount of vacancies produced during fatigue do neither form a sufficient density of agglomerates, nor does a sufficiently high fraction of the precipitates trap vacancies in order to create a measurable effect on the average positron lifetime when getting trapped there. The fact that fatigue crack tips can be visualized making use of focussed positron beams indicates that detectable damage is indeed produced but it is too localized to be measurable with a bulk method. On the other hand for a non-destructive testing method the precise knowledge of the fatigue crack initiation site is no practicable prerequisite.

Conclusions

In spite of the large turnover of vacancy-like defects during fatigue that also favours the formation of vacancy clusters, the determination of the average positron lifetime is not sufficient to detect the evolution of fatigue damage in the bulk material of industrial aluminium alloys. A fatigue induced modification of the positron trapping behaviour can only be observed unambiguously in front of the propagating fatigue crack tip by applying positron microbeams with sufficiently high spatial resolution [20–22]. Obviously such zones do not contribute with sufficient statistical weight to the large volume probed by the positrons with maximum energies of 2.5 MeV and 3.3 MeV that deeply penetrate into the aluminium alloys. In all examined cases trapping in precipitates dominates over trapping in fatigue-induced traps. In order to further investigate the utility of the non-destructive method of positron annihilation to monitor the evolution of fatigue damage also in aluminium alloys, more sophisticated methods like coincidence Doppler broadening spectroscopy might be applied to retrieve refined information on possible fatigue induced changes of the chemical environment of the positron trapping sites [16]. The required

minimum number of coincidence events necessitates however the use of stronger positron sources or much longer counting times and will probably limit its technological relevance for NDT purposes.

References

1. Puska MJ, Lanki P, Nieminen RM (1989) *J Phys: Condens Matter* 1:6081
2. Bischof G, Gröger V, Krexner G, Nieminen RM (1996) *J Phys: Condens Matter* 8:7523
3. Nieminen RM, Manninen MJ (1979) In: Hautojärvi P (ed) *Positrons in solids*, springer series topics in current physics. Springer-Verlag, Berlin, pp 143
4. Schulz PJ, Lynn KG (1988) *Rev Modern Phys* 60:701
5. Puska MJ, Nieminen RM (1994) *Rev Modern Phys* 66:841
6. Schaaff P, Holzwarth U (2005) *J Mater Sci* 40:6157
7. Hori F, Koike K, Oshima R (2005) *Appl Surf Sci* 242:304
8. Asoka-Kumar P, Hartley JH, Howell RH, Sterne PA, Akers D, Shah V, Denison A (2002) *Acta Mater* 50:1761
9. Müller I, Bennewitz K, Haaks M, Staab TEM, Eisenberg S, Lampe T, Maier K (2004) *Mater Sci Forum* 445–446:498
10. Kawaguchi Y, Nakamura N, Yusa S (2002) *Mater Trans* 43:727
11. Dupasquier A, Kögel G, Somoza A (2004) *Acta Mater* 52:4707
12. Macchi CE, Somoza A, Dupasquier A, Polmear IJ (2003) *Acta Mater* 51:5151
13. Massazza M, Riontino G, Dupasquier A, Folegati P, Ferragut R, Somoza A (2002) *Phil Mag Lett* 82:495
14. Somoza A, Dupasquier A, Polmear IJ, Folegati P, Ferragut R (2000) *Phys Rev B* 61:14454
15. Somoza A, Dupasquier A, Polmear IJ, Folegati P, Ferragut R (2000) *Phys Rev B* 61:14464
16. Calloni A, Dupasquier A, Ferragut R, Folegati P, Iglesias MM, Makkonen I, Puska MJ (2005) *Phys Rev B* 72:054112
17. Wider T, Maier K, Holzwarth U (1999) *Phys Rev B* 60:179
18. Hashimoto E, Ueda Y, Uematsu N, Iwami M, Kino T (1992) *J Phys Soc Jpn* 61:3799
19. Hidalgo C, González-Doncel G, Linderöth S, San Juan J (1991) *Phys Rev B* 45:7017
20. Zamponi Ch, Sonneberger St, Haaks M, Müller I, Staab T, Tempus G, Maier K (2004) *J Mater Sci* 39:6951
21. Egger W, Kögel G, Sperr P, Triftshäuser W, Bär J, Rödling S, Gudladt H-J (2004) *Mater Sci Eng A* 387–389:317
22. Egger W, Kögel G, Sperr P, Triftshäuser W, Bär J, Rödling S, Gudladt H-J (2003) *Z Metallkde* 94:687
23. Araki H, Fujita E, Nakata S, Shirai Y (1999) *Mater Sci Forum* 304–306:705
24. Abdel-Rahman MA, Abdallah MS, Badawi EA (2005) *Surf Rev Lett* 12:463
25. Badawi EA (2005) *Surf Rev Lett* 12:1
26. de Diego N, del Rio J, Romero R, Somoza A (1997) *Scripta Mater* 37:1367
27. Wider T, Hansen S, Holzwarth U, Maier K (1998) *Phys Rev B* 57:5126
28. Barbieri A, Hansen-Ilzhöfer S, Ilzhöfer A, Holzwarth U (2000) *Appl Phys Lett* 77:1911
29. Hansen S, Holzwarth U, Tongbhoyai M, Wider T, Maier K (1997) *Appl Phys A* 65:47
30. Mughrabi H (1978) *Mater Sci Eng* 33:207
31. Mughrabi H, Ackermann F, Herz K (1979) In: Fong JT (ed) *Fatigue mechanisms*, American Society for Testing and Materials, Special Technical Publication 675, Philadelphia, pp 69
32. Essmann U, Gössele U, Mughrabi H (1981) *Phil Mag A* 41:405

33. Basinski ZS, Basinski SJ (1989) *Acta Metall* 37:3275
34. Hoffmann E, Kleinert W, Schmidt W (1983) *Crystal Res Technol* 18:21
35. Wilhelm M (1981) *Mater Sci Eng* 48:91
36. Lee J-K, Laird C (1982) *Mater Sci Eng* 54:39
37. Annual Book of ASTM Standards (1992) *Metals test methods and analytical procedures*, vol 03.01, American Society for Testing and Materials, Philadelphia, PA, USA
38. Somieski B, Staab TEM, Krause-Rehberg R (1996) *Nucl Instr Meth Phys Res A* 381:128
39. Bennewitz K, Haaks M, Staab T, Eisenberg S, Lampe T, Maier K (2002) *Z Metallkde* 93:778
40. Dlubek G, Lademann P, Krause H, Krause S, Unger R (1998) *Scripta Mater* 39:893
41. Ferragut R, Somoza A (1999) *Phys Stat Sol (a)* 175:R1
42. Dlubek G, Krause H, Krause S, Unger R, Heyroth W (1998) *Phys Stat Sol (a)* 169:R11
43. Staab TEM, Zschech E, Krause-Rehberg R (2000) *J Mater Sci* 35:4667
44. Somoza A (1997) *Mater Sci Forum* 255–257:86
45. Schaefer H-E, Gugelmeier R, Schmolz M, Seeger A (1987) *Mater Sci Forum* 15–18:111
46. Haruyama O (1981) *Jap J Appl Phys* 20:1641
47. Dlubek G, Brümmer O, Krause R (1985) In: Jain PC, Singru RM, Gopinathan KP (eds) *Positron annihilation*. World Scientific Publ. Co., Singapore, pp 883
48. *Metals Handbook* (1979) 9th edn., vol 2 *Properties and selection: nonferrous alloys and pure metals*; American Society for Metals, Metals Park, Ohio 44073, USA, pp 28–132
49. *Atlas of Fatigue Curves* (1986) In: Boyer HE (ed) American Society for metals, Metals Park, Ohio 44073, USA, pp 319–390
50. Basini M, de Diego N, Del Rio J, Dupasquier A, Valli M, Abis S (1997) *Mater Sci Forum* 255–257:442
51. Ferragut R, Somoza A, Tolley A (2001) *Mater Sci Forum* 363–365:88
52. Schaefer H-E, Stuck W, Banhart F, Bauer W (1987) *Mater Sci Forum* 15–18:117
53. Ferragut R, Somoza A, Tolley A (1999) *Acta Metall* 47:4355
54. Danh NC, Rajan K, Wallace W (1983) *Metall Trans A* 14A:1843